CORE
Metadata, citation and similar papers at core.ac.uk

東北大学機関リポジトリ
TOUR
Tohoku University Repository

Synthesis and Electronic-Property Control of Cs-Encapsulated Single- and Double-Walled Carbon Nanotubes by Plasma Ion Irradiation

著者	畠山　力三
journal or publication title	Journal of Applied Physics
volume	102
number	3
page range	034309-1-034309-7
year	2007
URL	http://hdl.handle.net/10097/46582

doi: 10.1063/1.2768014

Synthesis and electronic-property control of Cs-encapsulated single- and double-walled carbon nanotubes by plasma ion irradiation

R. Hatakeyama and Y. F. Li[a)]
Department of Electronic Engineering, Tohoku University, Sendai 980-8579, Japan

(Received 22 March 2007; accepted 27 June 2007; published online 13 August 2007)

The synthesis of Cs-encapsulated single-walled carbon nanotubes (Cs@SWNTs) and double-walled carbon nanotubes (Cs@DWNTs) is realized by a plasma ion-irradiation method. Transmission electron microscopy observations confirm that chainlike and amorphous Cs fill SWNTs and DWNTs, respectively. The electronic transport properties of Cs@SWNTs and Cs@DWNTs are experimentally investigated at both room and low temperatures by fabricating them as the channels of field-effect transistor devices. Our results reveal that both Cs@SWNTs and Cs@DWNTs exhibit *n*-type semiconducting behavior at room temperature. The electronic properties of the Cs-encapsulated nanotubes can be controlled by adjusting the Cs filling levels during the plasma ion irritation process. At low temperatures, Coulomb blockade transport characteristics are observed for both encapsulated nanotubes, and the size of quantum dots formed in Cs@DWNTs is much smaller than that formed in Cs@SWNTs. More importantly, the *n*-type characteristics of Cs@SWNTs and Cs@DWNTs are found to remain stable, even in air, owing to Cs encapsulation. © *2007 American Institute of Physics*. [DOI: 10.1063/1.2768014]

I. INTRODUCTION

Single-walled carbon nanotubes (SWNTs) and double-walled carbon nanotubes (DWNTs) have shown great potential for applications in fabricating electronic devices since their discovery.[1–7] Experimental and theoretical studies have revealed that these nanotubes can be either metals or semiconductors, and their electrical properties can exceed those of the best metals and semiconductors known up to now. Pristine semiconducting SWNTs exhibit unipolar *p*-type behavior.[8] In contrast, pristine DWNTs are found to exhibit ambipolar semiconducting behavior due to their small band gap.[9] Subsequently, controlled chemical doping of SWNTs with electron donors or acceptors has been accomplished in a number of ways.[10–12] In order to modify the electronic properties of SWNTs, several methods, such as alkali metal doping, have been investigated in order to create *n*-type SWNTs, *p-n* or *p-n-p* junctions.[13–15] However, although alkali metals can act as good electron donors, alkali metals doped onto the SWNT surface cannot maintain their *n*-type behavior in air because of their inherent air instability. It remains an interesting question as to how to maintain their stable *n*-type behavior. In this regard, SWNTs encapsulating alkali metals are expected to be immune from the property degradation of inner alkali-metal atoms even under air exposure. In addition, compared with the case of SWNTs, only a few experimental studies related to the transport behavior of DWNTs are reported,[9,16,17] and little is known about the electronic properties of DWNTs encapsulating electron dopants, even though they have been predicated to form a better nanotube system than SWNTs.

In this work, a plasma ion irradiation method has been explored to control the encapsulation of Cs atoms inside SWNTs and DWNTs, and this method enables us to select the species of ionized atoms and control their flux or energy by changing the dc bias voltage applied to SWNTs or DWNTs. Our measured results suggest that air-stable *n*-type SWNTs or DWNTs can be created by Cs encapsulation. Moreover, *n*-type Cs-encapsulated DWNTs (Cs@DWNTs) are found to exhibit better characteristics in the mobility and on/off current ratio than those observed for Cs-encapsulated SWNTs (Cs@SWNTs) under the configuration of field-effect transistor (FET) devices.

II. EXPERIMENTAL DETAILS

A. Synthesis of Cs@SWNTs and Cs@DWNTs

Both SWNTs and DWNTs used here are prepared by an arc-discharge method. The raw SWNTs are purified by the hydrothermally initiated dynamic extraction (HIDE) method.[18] Raw DWNTs are purified by a combination of acid treatment and air oxidation before use. High-resolution transmission electronic microscopy observation confirmed that the as-synthesized DWNTs have high purity, and most of them have a uniform outer diameter of 4–5 nm. Both purified DWNTs and SWNTs are dispersed by a brief supersonic treatment in ethanol. Then, droplets of this suspension are dripped onto stainless steel substrates (15×15 mm^2) and dried. The production details of Cs plasma for irradiation-induced encapsulation are similar to those of other alkali-fullerene plasmas, as schematically illustrated in Fig. 1, and are described in details elsewhere.[19–21] When negative dc bias ($\phi_{ap}<0$) with respect to the grounded plasma-source electrode is applied to the substrate inserted into the plasma, positive Cs ions ($n_i\sim 1\times 10^{10}$ cm^{-3}, where n_i is ion density) are substantially accelerated by the plasma sheath in front of the substrate and finally irradiated onto the nanotubes, as schematically illustrated in Fig. 2. A major merit of using

[a)]Author to whom correspondence should be addressed; FAX: +81-022-263-9225; electronic mail: yfli@plasma.ecei.tohoku.ac.jp

 © 2007 American Institute of Physics

Downloaded 28 Mar 2010 to 130.34.135.83. Redistribution subject to AIP license or copyright; see http://jap.aip.org/jap/copyright.jsp

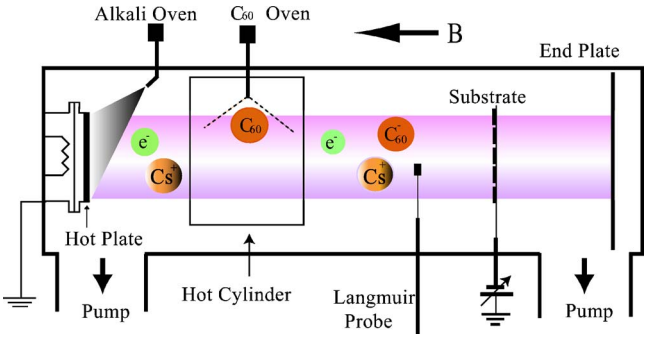

FIG. 1. (Color online) Schematic diagram of the experimental setup.

this method is that different filling levels of Cs@SWNTs and Cs@DWNTs can be obtained by adjusting the plasma irradiation time or applied bias voltage. In the present investigation, the plasma ion irradiation time is varied from 15 to 60 min. In addition, the application of different dc ϕ_{ap} (ranging from −25 to −150 V) during the same experimental time (60 min) is also carried out to synthesize different filling-level samples. Field emission transmission electron microscopy (FE-TEM) (Hitachi HF-2000) operated at 200 kV and having a point-to-point resolution of 0.23 nm is used for the structural characterization of purified and Cs-irradiated SWNTs and DWNTs. Energy dispersive x-ray spectrometry (EDX) (Noran Instruments) is utilized for chemical element detection.

B. Fabrication process of FET devices

In order to make FET devices, nanotube samples, including pristine SWNTs, DWNTs, and Cs@SWNTs and Cs@DWNTs with various filling levels, are first dispersed by supersonic treatment for over 9 h in *N*, *N*-dimethylformamide (DMF) solvent. Then the nanotube solution is spin-coated onto a FET substrate consisting of 63 pairs of Au electrodes, as schematically described in Fig. 3(a). Au electrodes with the thickness of 150 nm on a SiO_2 layer (thickness of 500 nm) are used as source and drain electrodes. The channel length between the source and drain electrodes is 500 nm. A heavily doped Si substrate is used as a backgate, and the backgate electrode is prepared by Al

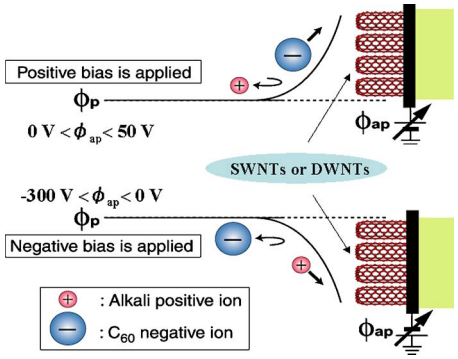

FIG. 2. (Color online) Schematic illustration of the plasma irradiation process. When positive dc bias, $0\ V < \phi_{ap} < 50\ V$, is applied, negative C_{60} ions can be accelerated toward SWNTs or DWNTs. On the contrary, when negative dc bias, $-300\ V < \phi_{ap} < 0\ V$, is applied, alkali positive ions such as Cs^+ are expected to be encapsulated into SWNTs or DWNTs.

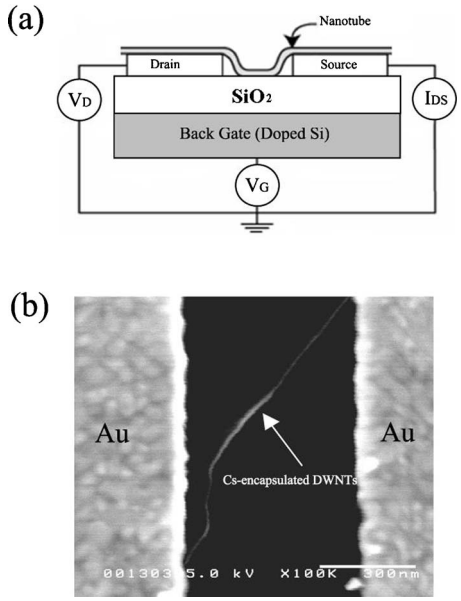

FIG. 3. (a) Schematic diagram of the nanotube-FET device. (b) SEM image of Cs@DWNT-FET device.

evaporation. Finally, a baking process at 400 K is carried out in air to remove the excess DMF solution and Cs attached to the outside of nanotubes. In this way, we can make nanotube-FET devices for electrical transport measurements. Nanotubes that bridge the two Au electrodes on the substrate are confirmed to exist by both atomic force microscopy (AFM) and scanning electron microscopy (SEM) observations. Figure 3(b) shows a typical SEM image of a FET device, where Cs@DWNTs crossing the two Au electrodes are clearly observed. Electronic transport properties of SWNT-FETs and DWNT-FETs are measured using a semiconductor parameter analyzer (Agilent 4155C) under both vacuum and air conditions. The source-drain current (I_{DS}) is systematically investigated as functions of gate bias (V_G) and source-drain bias (V_{DS}) measured at various temperatures ranging from room to low temperature.

III. RESULTS AND DISCUSSION

A. Morphology of Cs@SWNTs and Cs@DWNTs

Figure 4 shows high-resolution transmission electron microscopy (HRTEM) images for individual Cs@DWNT and Cs@SWNT, respectively, which were prepared by the plasma irradiation method. It is found that they display different morphologies under TEM observations. Helical chainlike Cs tend to be uniformly filled in an individual SWNT with a diameter of about 1.4 nm, as shown in Fig. 4(a), and the curved chainlike morphology of Cs seems to be periodically observed inside the SWNT. By comparison, owing to their structural rigidity and large diameter, DWNTs can support larger internal cavities than SWNTs. Amorphous Cs clusters, therefore, are clearly observed within an individual DWNT, as indicated in Fig. 4(b). The packing geometries of Cs in DWNTs may result from the overlap of many curved chainlike Cs arrangements, as illustrated in the inset of Fig. 4(b), which is different from that observed in Fig. 4(a) where only one line of Cs atoms fills the inside of SWNT. More-

Downloaded 28 Mar 2010 to 130.34.135.83. Redistribution subject to AIP license or copyright; see http://jap.aip.org/jap/copyright.jsp

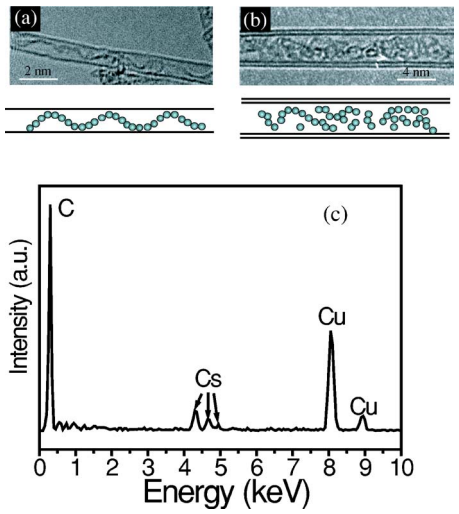

FIG. 4. (Color online) (a) TEM image of Cs@SWNT. Inset: chainlike Cs distributed along the nanotube. (b) TEM image of Cs@DWNT with an outer diameter ~4.8 nm and an inner diameter ~4.0 nm. Inset: packing arrangement of amorphous Cs in DWNT. (c) EDX spectrum of Cs@DWNTs indicating that the encapsulated material is Cs.

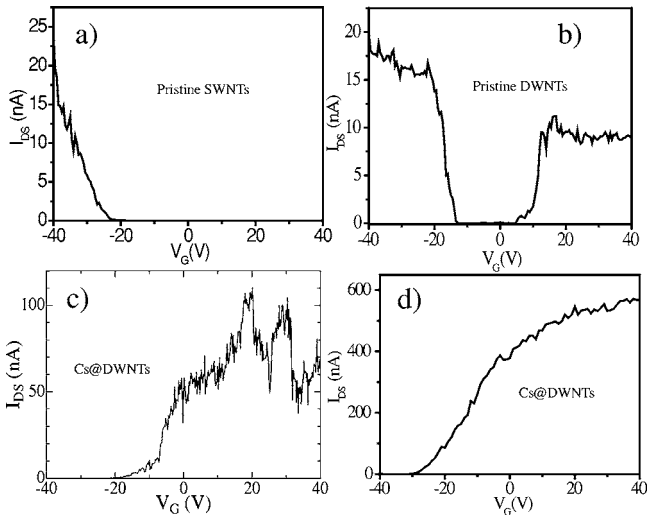

FIG. 5. The electronic transport properties of various nanotubes measured at room temperature in vacuum. (a) *p*-type pristine SWNTs measured at $V_{DS}=0.1$ V. (b) Ambipolar pristine DWNTs measured at $V_{DS}=0.1$ V. *n*-type (c) Cs@SWNT and (d) Cs@DWNT measured at $V_{DS}=1$ V, where the samples were prepared with $\phi_{ap}=-100$ V for 60 min.

over, EDX spectra have been taken of both Cs@SWNTs and Cs@DWNTs in order to confirm that the interior material is Cs. Figure 4(c) shows the EDX spectrum of Cs@DWNTs; several distinct peaks of Cs are seen, although they exhibit a relatively weak intensity. The large peak at low energy is due to the x ray of carbon. The Cu originates from the material of the TEM sample grid. Therefore, on the basis of the results of TEM observation, the EDX analysis is found to provide an indirect evidence of Cs encapsulation in SWNTs and DWNTs.

B. Electronic properties of Cs@SWNTs and Cs@DWNTs at room temperature

The electronic properties of SWNTs and DWNTs are observed to be significantly changed upon Cs encapsulation. For the purpose of comparison, we first present the electronic properties of pristine nanotubes. Figure 5(a) shows a typical I_{DS} vs V_G (I_{DS}-V_G) characteristic of a pristine SWNT-FET at room temperature with $V_{DS}=0.1$ V, indicating a clear *p*-type semiconducting behavior. In contrast, pristine DWNT-FETs exhibit obvious ambipolar transport behavior, and the characteristic of the I_{DS}-V_G curve at $V_{DS}=0.1$ V indicates that the device conducts either electrons or holes, depending on the gate bias, over a large range of gate voltages from −40 to 40 V, as shown in Fig. 5(b), and this is consistent with the previous result.[9] According to the typical results, the measured saturated conductance in the *p* channel is larger than that in the *n* channel for pristine DWNT-FETs. After Cs encapsulation, it is found that the FET device fabricated using either Cs@SWNT or Cs@DWNT exhibits a good *n*-type behavior. Figure 5(c) shows a typical I_{DS}-V_G characteristic of a Cs@SWNT-FET at room temperature with $V_{DS}=1$ V, showing a unipolar *n*-type behavior. This result evidently reveals that Cs atoms encapsulated inside SWNTs act as electron donors to SWNTs. The threshold voltage (V_{th}) for this *n*-type FET device is about −15 V. In the case of Cs@DWNTs, ambipolar DWNTs are found to be converted to *n*-type DWNTs by Cs encapsulation, as displayed in Fig. 5(d). The V_{th} measured at $V_{DS}=1$ V is about −30 V, which means that the carrier (electron) density along this Cs@DWNT is much higher than that along Cs@SWNTs, since the carrier density is directly proportional to the threshold gate voltage.[8] In addition, during our measurements, a high I_{on}/I_{off} ratio of about 10^5-10^6 is observed at various bias voltages for *n*-type Cs@DWNTs, which is much higher than that in the case of *n*-type Cs@SWNTs, which is of the order of 10^3-10^4.

To further assess the performance of Cs@SWNT-FETs, we investigate the output characteristic of I_{DS}-V_{DS} curves with V_{DS} ranging from 0 to 2 V by applying different gate voltages, as shown in Fig. 6(a). The measured results reveal that the conductance of the sample is significantly suppressed by decreasing the gate voltages from 40 V until the gate voltage reaches about 0 V, which further confirms that the FET device behaves as a *n*-type semiconductor. Figure 6(b) shows the I_{DS}-V_{DS} characteristics of Cs@DWNTs with V_G in the range of −30–40 V. In contrast to the case of Cs@SWNTs, the result indicates that conductance is suppressed until the gate voltage reaches −30 V, which also suggests that the electron density along *n*-type Cs@DWNTs is higher than that along *n*-type Cs@SWNTs. The details of electrical transport properties of Cs@SWNTs and Cs@DWNTs measured at room temperature are summarized in Table I. Here, the band gap is calculated for pristine nanotubes according to $E_g=2\alpha\gamma/d$ (Ref. 22) ($\alpha=0.142$ nm is the C–C bond length, $\gamma=2.5$ eV is the tight binding overlap integral, and d is the nanotube diameter, which is 1.4 and 4.5 nm for SWNT and DWNT, respectively). Although the band gap of DWNTs is smaller than that of SWNTs, Cs@DWNTs exhibit better characteristics in the mobility and on/off ratio than those of Cs@SWNTs. The mobility and subthreshold swing are calculated using $\mu=dI_{DS}/dV_G L\ln(2h/r)/(2\pi\varepsilon\varepsilon_0 V_{DS})$ (Ref. 8) and $S=dV_G/d\log_{10} I_{DS}$,[10] respectively, where $L=500$ nm is the

Downloaded 28 Mar 2010 to 130.34.135.83. Redistribution subject to AIP license or copyright; see http://jap.aip.org/jap/copyright.jsp

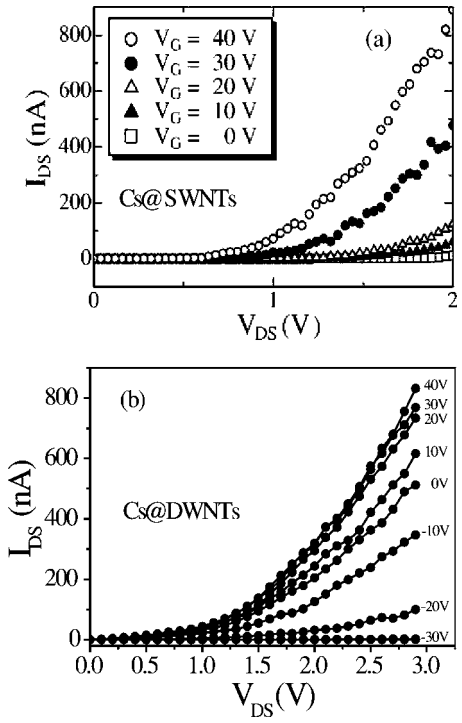

FIG. 6. (a) I_{DS}-V_{DS} output characteristics of Cs@SWNTs at V_G=40, 30, 20, 10, and 0 V. (b) I_{DS}-V_{DS} output characteristics of Cs@DWNTs measured for V_G varied in the range of −30–40 V in steps of 10 V at room temperature.

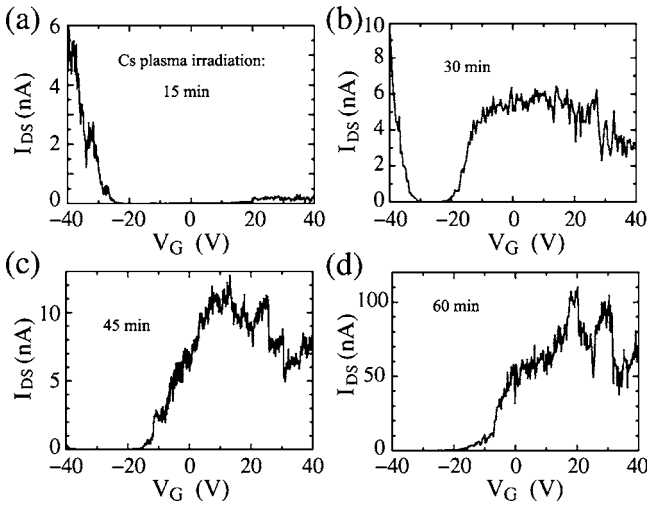

FIG. 7. Series of I_{DS}-V_G curves for Cs@SWNTs with various Cs ion irradiation times, measured at V_{DS}=1 V in vacuum. The amount of Cs irradiated to SWNTs was (a) $D=2.2\times10^4$/nm^2 (15 min), (b) 4.3×10^4/nm^2 (30 min), (c) 6.5×10^4/nm^2 (45 min), and (d) 8.6×10^4/nm^2 (60 min).

nanotube length between the drain-source electrodes, h =500 nm is the thickness of the oxide silicon layer, $\varepsilon\approx3.9$ is the average dielectric constant of the device, and r is the radius of nanotubes. The observed excellent characteristic of DWNTs is possibly due to the larger contact area that results in the formation of the Ohmic contact with Au electrodes. For SWNTs, only the Schottky contact is considered to be formed owing to their small diameter, according to recent works.[23,24]

One of advantages of using the plasma irradiation method is that the filling level of Cs atoms inside SWNTs or DWNTs might be controlled by adjusting the ion irradiation time or applied dc bias voltages ϕ_{ap}.[25] Variations in electronic properties of Cs@SWNTs prepared by changing the plasma irradiation time from 15 to 60 min are presented in Fig. 7. The amount of injected Cs atoms per area D is simply estimated by $D=tI/SC$, where t, $S(1.5\times1.5\ \text{cm}^2)$, and $C(1.6\times10^{-19}\ \text{C})$ are the irradiation time, the substrate size, and the electron charge of a Cs ion, respectively. During the plasma irradiation process, the measured current flowing to the substrate with SWNTs is about I=860 μA with ϕ_{ap}= −100 V. Thus the four samples of Cs@SWNTs shown in Figs. 7(a)–7(d) were prepared by the Cs ion irradiation process, during which the concentration of Cs^+ was about 2.2 $\times10^4$, 4.3×10^4, 6.5×10^4, and 8.6×10^4 Cs ions per nm^2, respectively. Obviously, the ambipolar semiconducting behavior remains in the range of low filling levels, as seen in Figs. 7(a)–7(c). A threshold gate voltage for p-type conductance appears to shift more negatively from −22.2 to −35.6 V, and the conductance region of n-type gradually increases with increasing total amount of irradiated Cs atoms. Finally, Cs@SWNTs change to show complete n-type behavior, as described in Fig. 7(d).

Moreover, by changing the applied dc bias voltages ϕ_{ap} different nanotube samples with different filling levels are also obtained, as shown in Fig. 8. Figure 8(a) gives the I_{DS}-V_G characteristic for a Cs@DWNT-FET device, in which the sample is prepared with ϕ_{ap}=−25 V. It can be seen that although the FET device still retains its ambipolar behavior at a low Cs filling level the ratio of the saturated conductance in the n channel to that in the p channel represents a relative increase compared with that of pristine DWNTs. Furthermore, for the sample of Cs@DWNTs prepared with ϕ_{ap}= −50 V, the ambipolar pristine DWNTs tend to be converted into n-type DWNTs with little conductance remaining in the p channel for gate voltages less than −30 V, as indicated in Fig. 8(b). It is obvious that the amount of encapsulated Cs, namely, the charge transfer from Cs atoms to DWNTs, is responsible for the formation of n-type DWNTs. It is important to note that at a low filling level p-n junctions are occasionally observed to be formed in Cs@DWNTs that are partially filled with Cs and some part of the nanotube remains empty. Furthermore, when the negative ϕ_{ap} is greater than −100 V, corresponding to a high Cs filling level, ambipolar

TABLE I. Electronic properties of n-type Cs@SWNTs and n-type Cs@DWNTs.

Samples	Band gap E_g (eV)	On/off ratio (I_{on}/I_{off})	Mobility μ (cm^2/V s)	Subthreshold swing S (V/decade)	Threshold voltage V_{th} (V)
Cs@SWNTs	0.50	10^3–10^4	0.5–1.0	5–10	from −15 to −30
Cs@DWNTs	0.16	10^5–10^6	1.6–2.0	5–10	from −25 to −35

Downloaded 28 Mar 2010 to 130.34.135.83. Redistribution subject to AIP license or copyright; see http://jap.aip.org/jap/copyright.jsp

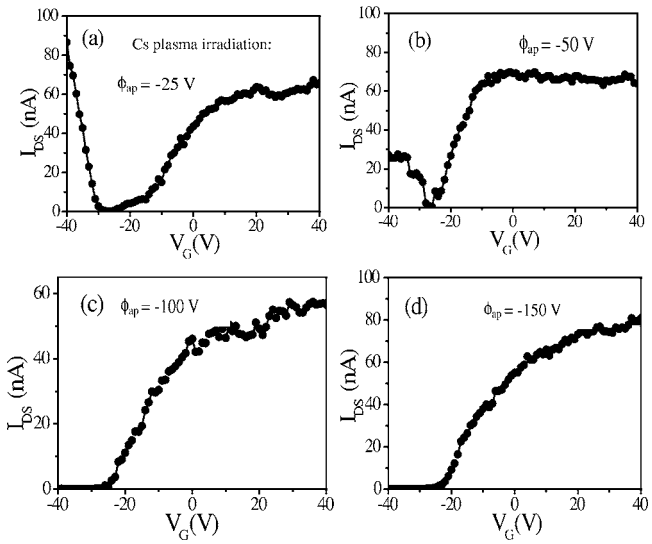

FIG. 8. Electrical transport properties of Cs@DWNTs prepared at different dc bias voltages with the same plasma irradiation time (60 min): (a) ϕ_{ap}= −25 V, (b) ϕ_{ap}=−50 V, (c) ϕ_{ap}=−100 V, and (d) ϕ^{ap}=−150 V.

DWNTs can be completely converted into unipolar *n*-type DWNTs, as shown in Figs. 8(c) and 8(d), respectively. It is worth mentioning that the above-observed results are based on our numerous measurements. Therefore, we can conclude that the semiconducting properties of Cs@SWNTs and Cs@DWNTs depend on the plasma irritation time and the negative dc bias voltage, i.e., the conversion of the nanotube property may possibly be controlled by the plasma irradiation method.

C. Electronic properties of Cs@SWNTs and Cs@DWNTs at low temperatures

At low temperatures, on the other hand, the transport characteristics observed for *n*-type Cs@SWNTs and Cs@DWNTs are dominated by Coulomb blockade phenomena, suggesting that quantum dots are created in these nanotubes. In particular, in our case, we can gain further insight into the size of formed quantum dots in comparison with Cs@SWNTs and Cs@DWNTs since they are different from each other in structure. Figures 9(a) and 9(b) show the evolution of the I_{DS}-V_G characteristic for *n*-type Cs@SWNTs and Cs@DWNTs, respectively, measured at V_{DS}=10 mV at various temperatures. The conductance of both the devices is monotonically reduced with decreasing temperature. The I_{DS}-V_G curves for Cs@SWNTs exhibit diamond structures below 40 K in the regime of 23 V$<V_G<$30 V, which is a signature of Coulomb blockade, as shown in Fig. 9(a). The average gate periodic spacing ΔV_G is estimated to be about 0.5 V for the case of Cs@SWNTs. The average ΔV_G of about 5.2 V is found in the regime of 0 V$<V_G<$40 V in Fig. 9(b) for the case of Cs@DWNTs, which is ten times larger than the case of Cs@SWNTs. Since the value of ΔV_G is indicative of the size of quantum dots, we can roughly estimate the dot size using a equation $\Delta V_G/e \approx \ln(2L/d)/2\pi\varepsilon\varepsilon_0 L$,[26] where L, d, and ε are the dot size, diameter of nanotubes, and dielectric constant, respectively. However, since the 500-nm-thick oxide backgate is used for

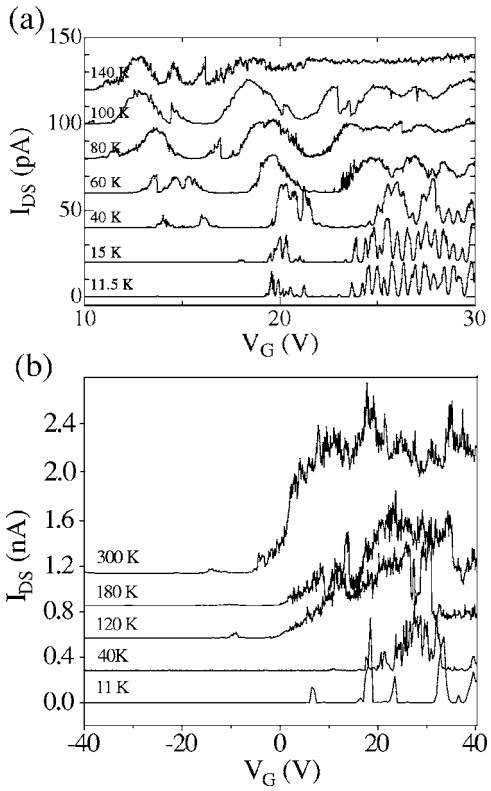

FIG. 9. (a) I_{DS}-V_G characteristics of *n*-type Cs@SWNTs measured at V_{DS} =10 mV in the temperature range from 140 to 11.5 K, indicating that the Coulomb blockade phenomenon appears at temperatures below 15 K and the average gate periodic spacing ΔV_G is 0.5 V. (b) I_{DS}-V_G characteristics of *n*-type Cs@DWNTs measured at V_{DS}=10 mV in the temperature range from 300 to 11 K, indicating that the observed average gate period is ΔV_G =5.2 V.

FET device fabrication, the efficiency of the gate voltage is estimated to be about 10% or less. Using 10% efficiency ΔV_G (about 0.05 V), d=1.4 nm, and ε=3.9, the size of quantum dots in Cs@SWNTs is calculated to be about L =200 nm. By comparison, small quantum dots with L =12 nm seem to be created inside Cs@DWNTs. Obviously, the quantum dot sizes for both the samples are much smaller than 500 nm for the nanotube length between the drain-source electrodes. Furthermore, we compared the above transport characteristics with those of pristine SWNTs and DWNTs measured at low temperatures. As a result, the Coulomb oscillation phenomenon is also observed for pristine SWNTs (see supporting information). This can be attributed to native defects on SWNTs, which form tunnel barriers at low temperatures.[27] However, the observed average ΔV_G for pristine SWNTs at 12.5 K is found to be about 0.13 V, which is much smaller than that of Cs@SWNTs. In the case of pristine DWNTs, no Coulomb oscillation is observed, suggesting that they represent an ideal nanotube system even at low temperatures (see supporting information). Our results described above evidently reveal that the Coulomb oscillation transport behavior of Cs@SWNTs and Cs@DWNTs originates from the Cs-encapsulation profiles inside SWNTs and DWNTs, and the potential barriers are possibly a result of the inhomogeneous Cs distribution along the nanotubes. The degree of inhomogeneous encapsulation may be directly related to the diameter of nanotubes. Because of the large

Downloaded 28 Mar 2010 to 130.34.135.83. Redistribution subject to AIP license or copyright; see http://jap.aip.org/jap/copyright.jsp

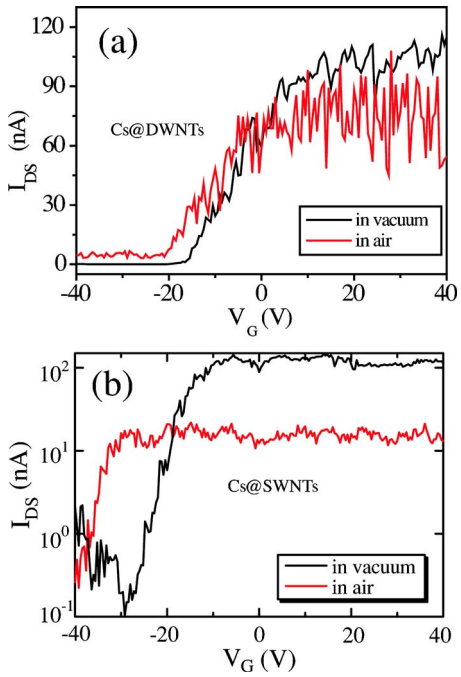

FIG. 10. (Color online) (a) I_{DS}-V_G characteristics of *n*-type Cs@DWNT measured at V_{DS}=1 V with Au drain-source electrodes in vacuum (black line) and in air (red line), respectively. (b) I_{DS}-V_G characteristics of *n*-type Cs@SWNT measured at V_{DS}=6 V with Ti drain-source electrodes in vacuum (black line) and in air (red line), respectively.

diameter, more homogeneous Cs encapsulation seems to be achieved in DWNTs rather than SWNTs, as observed in Fig. 4(a), and may result in the formation of small quantum dots.

D. Air stability of *n*-type Cs@SWNTs and Cs@DWNTs

Air-stable *n*-type nanotube-FET devices are of significant importance in their real commercial applications. However, previous investigations revealed that *n*-type SWNTs synthesized by doping alkali metals are not at all stable in air. The main reason might be that most doped alkali metals only attach to the outside of nanotubes, and they are easily oxidized in air. In our case, the shell of nanotubes can protect well the encapsulated Cs against oxidation in air, and therefore, air-stable *n*-type characteristics can be obtained under the appropriate conditions of charge transfer among the nanotube, Cs, and air (oxygen) atmosphere. Figure 10(a) shows I_{DS}-V_G characteristics for *n*-type DWNTs measured at V_{DS}=1 V in both vacuum and air (after exposure to air for over 1 h), respectively. Obviously, the *n*-type behavior remains in air although noiselike fluctuations appear to exist in the I_{DS}-V_G curve and the on/off ratio is appreciably degraded compared with the data measured in vacuum. The current drop can possibly be explained by the contact between the nanotubes and electrodes, which is unsuitable for the moment in the case of using Au for drain-source electrodes.

In the case of Cs@SWNTs, on the other hand, the output current I_{DS} vs V_{DS} completely vanishes for any V_G once the Cs@SWNT-FET device is exposed to air. However, when the system is pumped down to below 10^{-3} Torr, we can obtain almost the same characteristic of I_{DS}-V_G curves as before exposure to air. The possible reason for the above phenomenon may be that the charge transfer effect from SWNTs to oxygen diminishes the *n*-type characteristic of Cs@SWNTs in air. Moreover, the contact between SWNTs and the Au electrodes is less firm than that between DWNTs and the Au electrodes, which is considered to be due to the diameter difference between SWNTs and DWNTs. In addition, the structural merit of DWNTs cannot be ruled out, since much fewer structure defects are generated on DWNTs as compared with the case of Cs@SWNTs, and their two carbon layers can efficiently prevent the encapsulated Cs from being oxidized.

In order to improve the situation on the air-stable characteristics, Ti instead of Au is used for electrodes in our experiments with Cs@SWNTs. Compared with our previous FET fabrication process, an additional annealing process at about 1000 °C in high vacuum is performed to form titanium carbide between the nanotube and Ti electrodes. Figure 10(b) shows the I_{DS}-V_G characteristics of (measured with V_{DS} =6 V using Ti as electrodes) for Cs@SWNTs at room temperature in both vacuum and air, respectively. The behavior of I_{DS}-V_G in vacuum (black line) indicates that the Cs@SWNT-FET device acts as a *n*-type semiconductor. After this Cs@SWNT-FET is exposed to air, its I_{DS}-V_G characteristic (red line) still persists even in air. To confirm this air-stable characteristic, the first measurement is carried out in vacuum, and then the device is exposed to air and measured during our experiments. After that, the system is pumped and the device is measured again in vacuum. Such repeated measurements are performed many times to confirm the electrical properties of Cs@SWNT-FET in air and in vacuum. During each measurement, the characteristics of I_{DS}-V_G represent a recovered property and no noiselike fluctuation exists. This result indicates definitively that excellent air-stable *n*-type nanotubes are obtained. Thus, our series of experimental results confirm that the reactive Cs atoms are protected against oxidation by the carbon layers because the Cs atoms are encapsulated inside DWNTs and SWNTs.

IV. CONCLUSION

The electronic transport properties of Cs@SWNTs and Cs@DWNTs prepared by the plasma ion irradiation method were investigated in detail in the ambient temperature range from low to room temperatures. Both Cs@SWNTs and Cs@DWNTs were verified to display a *n*-type behavior, even in air. In particular, Cs@DWNTs exhibited better characteristics than those observed for Cs@SWNTs. By varying the plasma irradiation time or dc bias voltage of the tube-coated substrate in plasmas, electrical transport properties of Cs@SWNTs and Cs@DWNTs can controllably be modified by Cs encapsulation at different filling levels. At low temperatures, Coulomb oscillations were observed to arise in the transport characteristics of both Cs@SWNTs and Cs@DWNTs, and the results demonstrated that quantum dots were formed in the nanotubes owing to Cs encapsulation. The size of quantum dots estimated for Cs@DWNTs is found to be much smaller than that estimated for Cs@SWNTs because of an inhomogeneity difference of Cs encapsulation.

Downloaded 28 Mar 2010 to 130.34.135.83. Redistribution subject to AIP license or copyright; see http://jap.aip.org/jap/copyright.jsp

ACKNOWLEDGMENTS

We are grateful to Professor K. Tohji and Mr. K. Motomiya for their help in TEM observation and to Mr. T. Izumida for collaboration. This work was supported by Tohoku University 21st Century Center of Excellence (COE) Program, Research Fellowship of Japan Society for the Promotion of Science (JSPS), and JSPS-CAS Core-University Program on Plasma and Nuclear Fusion.

[1]S. J. Tans, A. R. M. Verschueren, and C. Dekker, Nature (London) **393**, 49 (1998).
[2]T. W. Odom, H. Jin-Lin, P. Kim, and C. M. Lieber, Nature (London) **391**, 62 (1998).
[3]M. Bockrath, D. H. Cobden, P. L. McEuen, N. G. Chopra, A. Zettl, A. Thess, and R. E. Smalley, Science **275**, 1922 (1997).
[4]J. Kong, C. Zhou, E. Yemilmez, and H. J. Dai, Appl. Phys. Lett. **77**, 3977 (2000).
[5]T. Takenobu, T. Takano, M. Shiraishi, Y. Murakami, M. Ata, H. Kataura, Y. Achiba, and Y. Iwasa, Nat. Mater. **2**, 683 (2003).
[6]S. Wang and M. Grifoni, Phys. Rev. Lett. **95**, 266802 (2005).
[7]M. Kociak, K. Suenaga, K. Hirahara, Y. Saito, T. Nakahira, and S. Iijima, Phys. Rev. Lett. **89**, 155501 (2002).
[8]R. Martel, T. Schmidt, H. R. Shea, T. Hertel, and Ph. Avouris, Appl. Phys. Lett. **73**, 2447 (1998).
[9]T. Shimada, T. Sugai, Y. Ohno, S. Kishimoto, T. Mizutani, H. Yoshida, T. Okazaki, and H. Shinohara, Appl. Phys. Lett. **84**, 2412 (2004).
[10]A. Javey, R. Tu, D. B. Farmer, J. Guo, R. G. Gordon, and H. J. Dai, Nano Lett. **5**, 345 (2005).
[11]T. Izumida, G.-H. Jeong, Y. Neo, T. Hirata, R. Hatakeyama, H. Mimura, K. Omote, and Y. Kasama, Jpn. J. Appl. Phys., Part 1 **44**, 1606 (2005).
[12]Y. F. Li, R. Hatakeyama, T. Kaneko, T. Izumida, T. Okada, and T. Kato, Appl. Phys. Lett. **89**, 083117 (2006).
[13]C. Zhou, J. Kong, E. Yenilmez, and H. J. Dai, Science **290**, 1552 (2000).
[14]J. Kong, J. Cao, and H. J. Dai, Appl. Phys. Lett. **80**, 73 (2000).
[15]J. Kong and H. J. Dai, J. Phys. Chem. B **105**, 2890 (2001).
[16]Y. F. Li, R. Hatakeyama, T. Kaneko, T. Izumida, T. Okada, and T. Kato, Nanotechnology **17**, 4143 (2006).
[17]Y. F. Li, R. Hatakeyama, T. Kaneko, T. Izumida, T. Okada, and T. Kato, Appl. Phys. Lett. **89**, 093110 (2006).
[18]K. Tohji *et al.*, Nature (London) **383**, 679 (1996).
[19]G.-H. Jeong, R. Hatakeyama, T. Hirata, K. Tohji, K. Motomiya, N. Sato, and Y. Kawazoe, Appl. Phys. Lett. **79**, 4213 (2001).
[20]G.-H. Jeong, T. Hirata, R. Hatakeyama, K. Tohji, and K. Motomiya, Carbon **40**, 2247 (2002).
[21]R. Hatakeyama, T. Hirata, and G.-H. Jeong, Plasma Sources Sci. Technol. **13**, 108 (2004).
[22]L. Francois and T. A. Alen, Phys. Rev. Lett. **97**, 026804 (2006).
[23]Z. Chen, J. Appenzeller, J. Knoch, Y. Lin, and Ph. Avouris, Nano Lett. **5**, 1497 (2005).
[24]W. Kim, A. Javey, R. Tu, J. Cao, Q. Wang, and H. J. Dai, Appl. Phys. Lett. **87**, 173101 (2005).
[25]T. Izumida, R. Hatakeyama, Y. Neo, H. Mimura, K. Omote, and Y. Kasama, Appl. Phys. Lett. **89**, 093121 (2006).
[26]A. Bezryadin, A. R. M. Verschueren, S. J. Tans, and C. Dekker, Phys. Rev. Lett. **80**, 4036 (1998).
[27]H. W. C. Postma, T. Teepen, Z. Yao, M. Grifono, and C. Dekker, Science **293**, 76 (2001).

Downloaded 28 Mar 2010 to 130.34.135.83. Redistribution subject to AIP license or copyright; see http://jap.aip.org/jap/copyright.jsp